Type of the Paper (Article, Review, etc.)

Determination, Manufacturing and application of a nanoparticle lead ion-selective electrode as a sensor in flow injection systems

Shatha Y. Al-Samarrai[1]*

[1] Chemistry Department, College of Science, Tikrit University, Iraq.
*Corresponding Author: dr.shatha81@tu.edu.iq

Received date: 05/12/2023; Accepted date: 06/01/2024; Published date: 10/01/2024

Abstract:

This study involves the construction of ion-selective electrodes for the determination of lead (II) ions and their utilization as sensors in a flow-injection analysis (FIA) system. The electrode was constructed using a simple environmentally friendly method from a green tea extract, and a Lead acetate solution of the cited ions as a cylindrical disc. A vertical, side-to-side cylinder, the whole is created in its centre and another lateral hole is created for the electrical attachment of the electrode, so the prepared electrode is suitable for use with the FIA system. The electrode was studied surface properties and characteristics of this electrode were analysed using X-ray diffraction and Fourier-transform infrared spectroscopy (FTR). via selection of the optimum conditions (i.e. linear calibration range, lowest Nernstian response, lowest detection limit, degree of dilution, and precision and accuracy of their analytical uses). Electrode which gave the best Nernstian response1.00×10^{-1} to 1.00×10^{-10} M, a correlation coefficient of 0.9980, with lower Nernstian response of 1×10^{-10} M and detection limit of 1×10^{-11} M. The sampling rate was 120 samples per hour the calculated time of the contact of the sample with the electrode surface is 6 seconds and the degree of dilution is 2.37625.

Keywords: ISEs; Lead; Nanoparticle; Sensor.

1. Introduction

Due to their distinct electrochemical characteristics and prospective uses in a variety of disciplines, such as environmental monitoring and medical diagnosis, lead nanoparticle electrodes have grown in popularity over the past several years. Lead nanoparticle electrodes are used in flow injection analysis (FIA), which uses them as sensors that measure changes in the current or potential at the electrode in response to the presence of an analyte in the sample solution. This is one of the most promising uses for lead nanoparticle electrodes (1).
There are many advantages of using Lead nanoparticle electrodes in FIA compared to conventional electrodes, such as improved sensitivity and selectivity, low cost, ease of manufacture and switching Due to its specific capacitance due to size and surface area to number ratio, Lead nanoparticles are ideal for electrochemical analysis and sensing (2).
Lead nanoparticle electrodes have been investigated in recent years to improve their synthesis and evaluate their effectiveness in FIAs for the detection of various analytes, such as heavy metals, organic contaminants and biomarkers and have proven their effectiveness. scientists have explored the use of environmentally friendly synthetic materials such as plant extracts to

make Lead nanoparticle electrodes and have proven their effectiveness in environmental conditions in the sight of our polluted surroundings (3).
Using Lead nanoparticle electrodes in FIA can detect a wide range of analytes with good sensitivity and selectivity, a rapidly growing field Lead nanoparticle electrodes prove to be a viable technology for electrochemical sensing and analysis, despite drawbacks much like the need for innovation and change strategic planning (4,5). Green tea (Camellia sinensis) has also been described as a potential source of Lead nanoparticles. Green tea catechins have been shown to act as a reducing agent, dissolving Lead ions to form Lead nanoparticles (6).
Compared to conventional methods, using green tea as a reducing agent has many advantages such as low toxicity, biodegradability, and low-cost Using tea green plays a role in the production of Lead nanoparticles to reduce hazardous waste generation and environmental impact a synthetic approach (7). Additionally, the high stability and electrical conductivity of Lead nanoparticles made from green tea were demonstrated to be better to those made using traditional techniques. (8,9). However, to prevent contamination of the final product and to guarantee the sustainability of the entire process, strict supervision of the raw material is required (10).
The use of the green chemistry method in Lead nanoparticle electrosynthesis as a sensor for flow injection analysis (FIA) aims to make the process environmentally benign, cost-effective and safe, and in lead nanoparticle electrical vehicles there is performance Improvement. This process reduces the use of hazardous chemicals and waste and can lead to more sustainable raw materials. Lead nanoparticle electrodes have high sensitivity and selectivity for various analytes, making them a valuable tool in FIA applications. The green chemistry approach can further enhance these properties, making lead nanoparticle electrodes a more useful tool for FIA.

2. Materials and Methods

2.1. Apparatus.

An analogy peristaltic pump made by ISMATEC SA, a Swiss subsidiary of IDEX Corporation, was used to construct the FIA system. This high-quality pump was specifically designed with PVC tubes that had a diameter of 0.5 mm, enabling precise and efficient pumping. To introduce the solutions into the system, an RHEODYNE 7125 injection valve from the USA was seamlessly connected to the pump. For reliable and accurate measurements, a HANNA Calomel electrode (HI1144B) sourced from the USA was employed as the reference electrode. pH values, an essential parameter for the experiments, were carefully monitored using a JENWAY BL Meter (model 3310) imported from the UK. The appearance and crystal arrangement of the substances were examined through the utilization of a field emission scanning electron microscope (SEM, ZEISS EVO 15). The FT-IR spectra were captured using the KBr pellet technique with a SHIMADZU-8400 spectrometer. Additionally, an X-ray diffractometer (XRD, Phillips PW3040/60) was employed in the analysis. Throughout the experiments, a controlled environment was maintained at room temperature, precisely set at 27.0 ± 2.0 °C to ensure consistent and reproducible results.

2.2. Solutions and reagents.

The chemicals were incredibly pure and didn't undergo any more purification steps prior to being used. The solutions were prepared using potassium nitrate, ammonium acetate, lead acetate, perchlorate sodium, and double-distilled water with a conductivity range of 0.2 to 0.6 S. Standard Lead Acetate Solution (0.1M), this solution was prepared by dissolving 3.2529 g of lead acetate trihydrate diluted to 100mL with distilled water in a volumetric flask. And the Carrier current 0.1 M were prepare from a 0.1 Molar solution was created by dissolving the amount of Perchlorate sodium, ammonium acetate, and potassium nitrate in a volumetric flask that was provided with 100 mL of distilled water.

2.3. Procedures.

After being dried, 10 grams of green tea (Camellia sinensis) leaves were heated for 15 minutes at 70 °C in 100 mL of deionized water. The extract was then filtered from the leaves and used immediately. There were several phases involved in the green synthesis process used to create Pb nanoparticles (Pb-NPs). First, 100 mL of aqueous green tea extracts were combined with 0.1 M lead acetate. The mixture was then agitated for an hour at a temperature of 800C. After the desired reaction time, the solution was cooled to room temperature. Subsequently, centrifugation at 2000 rpm for 5 minutes was conducted to separate the lead nanoparticles (Pb-NPs), leading to the development of precipitates. This step was essential for isolating the Pb-NPs and resulted in the formation of visible precipitates in the solution. These precipitates were meticulously collected, and 700C drying was then performed (11), Figure 1 provides an illustration of this process.

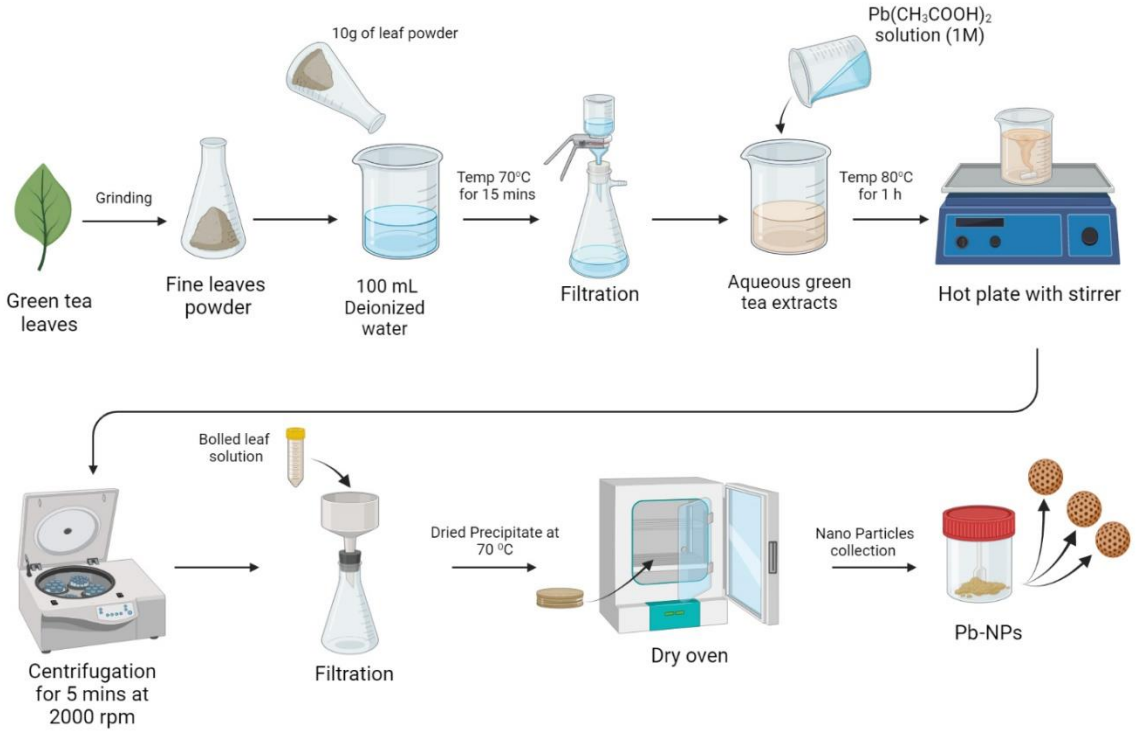

Figure 1: A graphic demonstrating the production of lead nanoparticles from green tea extract.

Using a ceramic mortar, the material was homogenized until it created a very fine powder. The powder was subsequently screened using a sieve with holes 300 micrometers in diameter. Using a pharmaceutical pill-making machine, the substance was then squeezed into the shape of hard disks. The resulting hard disks were 0.6 mm thick, 13 mm in diameter, and 0.9 grams in weight. The disk was then vertically punctured, resulting in a 1.5 mm diameter hole that ran the length of the disk. A side hole was also drilled into the disk to accommodate an electrical connection wire. It is vital to notice that the side hole's depth did not surpass 2 mm.

Insulating materials were utilized to prevent any contact between the electrode and the surrounding surfaces, except through the wire, to ensure electrical insulation. Figure 2 shows a visual representation of the created electrode.

A wire is 4 cm in length was prepared. One end of the wire was securely fastened to the side of a Pb-NPs (Lead Nanoparticles) produced disk.

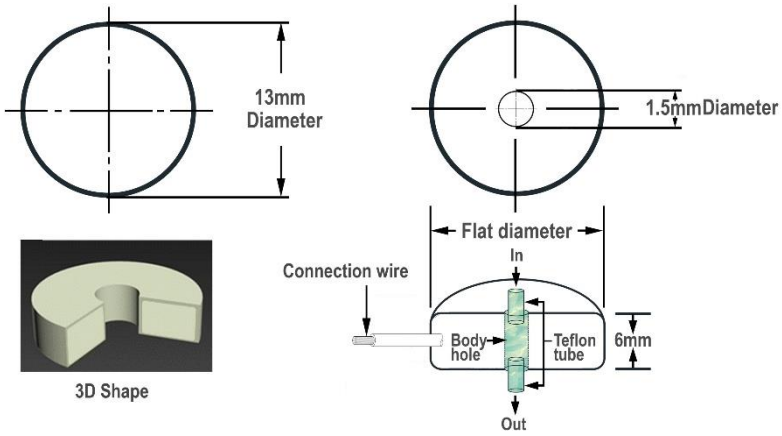

Figure 4: A design diagram of the Pb-NPs electrode.

3. Results and discussion.

3.1. Utilization of Electrode

A constructed electrode was used as a working electrode in the first experiment to measure potential differences using the FIA technique. As indicated in Figure 3, the electrode was attached to a simple manifold unit. The tank's carrier solution current was continually injected at a steady flow rate into a specific conduit. This flow rate could be controlled continuously by a peristaltic pump to the rotary injection valve, and from there, to the mixing tube. The working electrode and the reference electrode (calomel electrode) were then connected to a potentiometer, which expressed the voltage response in height. This potentiometer was then connected to a paper recorder to record the potential difference between the two electrodes.

The calomel electrode was placed inside a cylindrical plastic container of suitable capacity, with two openings for the carrier solution to enter and exit. The exit hole was slightly higher than the sensitive part of the electrode to ensure electrical contact. To inject the sample into the carrier current solution, the injection rotary valve was rotated to the injection site with constant accuracy and speed. The sample then entered the flow system and was transported by the carrier current after passing through the mixing tube to the specially manufactured guide electrode and then to the reference electrode before being recorded on the paper recorder. Under optimal conditions, the height of the tip was proportional to the concentration of the substance being analyzed (analyte). After the study of the electrode properties was completed, a stream of distilled water was passed through the manifold unit at the same recorded flow rate for at least five minutes. This was done to ensure that the manifold unit was thoroughly washed and ready for subsequent use.

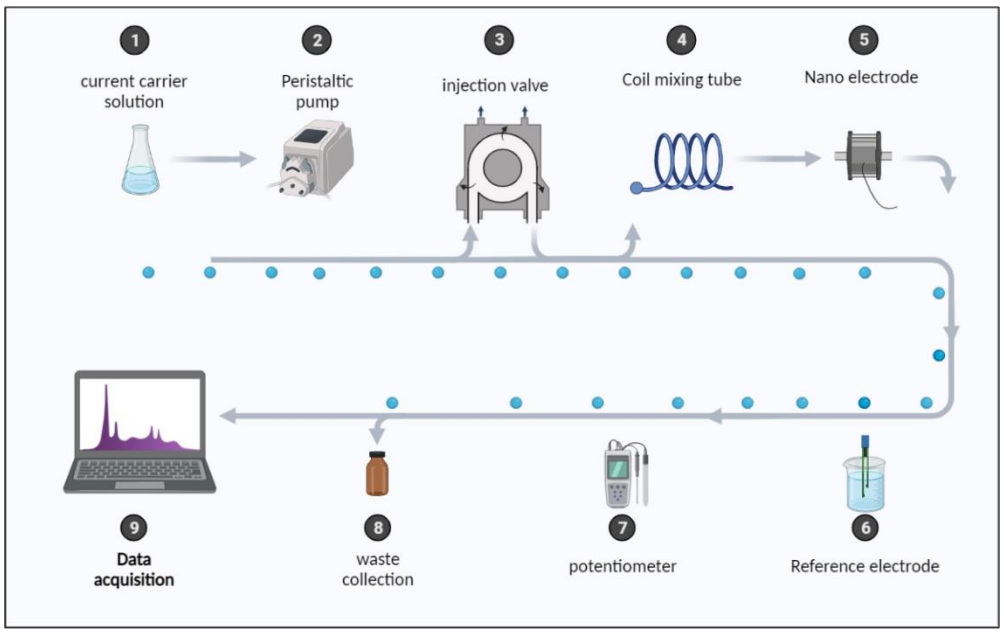

Figure 3: A visual diagram illustrating the Flow Injection Analysis system.

3.2. Spectroscopic characterization of Pb nanoparticles

3.2.1. FT-IR spectroscopy.

The FT-IR spectra shows in Figure 4 of Pb nanoparticles between 4000-400 cm^{-1}. Different bands connected to polyphenolic chemicals are responsible for the large peaks connected to hydroxyl groups that are visible at 3545.62 cm^{-1} in the spectra of lead nanoparticles. (12-15). Notably, a pronounced IR absorption at 2387.65 signifies stretching vibrations resulting from C-O bonds. This finding suggests that throughout the Pb $(CH_3COO)_2$ preparation process, certain C-O groups were integrated into the Pb nanoparticles .

Additionally, the stretch-bending vibration of O-H bonds is represented by the peak at 1060.22 cm^{-1}. Furthermore, the presence of Pb-O and Pb-O-Pb bonds is indicated by the absorption peaks found at 662.67 and 685.56 cm^{-1}, respectively. The peaks falling within the 400-800 cm^{-1} range are indicative of metal-oxygen stretching interactions.

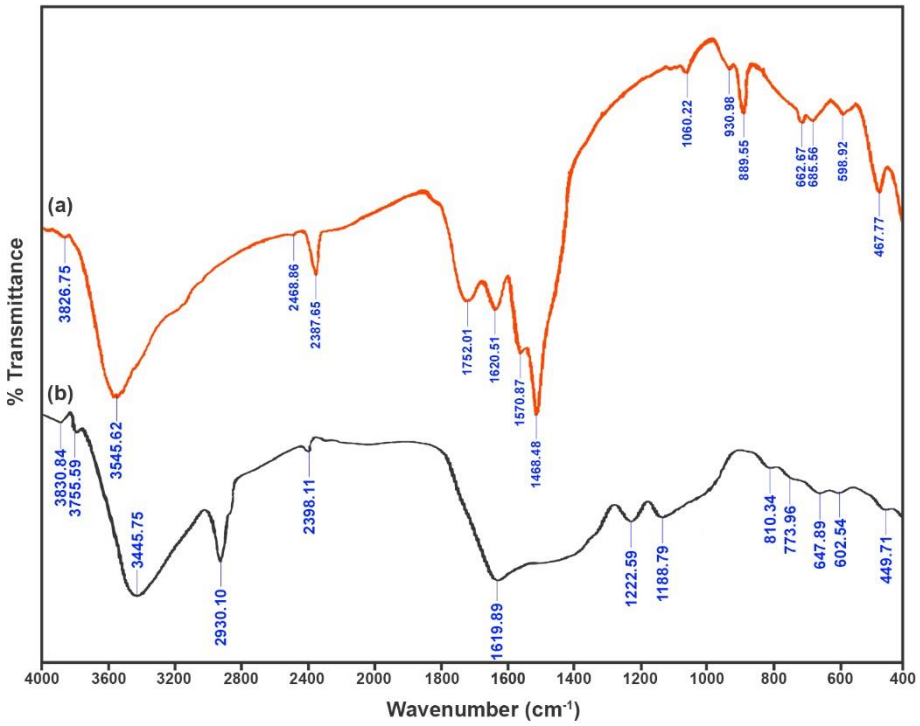

.**Figure 4:** FT-IR spectrum of (a) synthesized Pb-NPs. and (b) green tea extract

3.2.2. Diffraction of x-rays

Figure 5 shows the results of X-ray diffraction (XRD) for Pb nanoparticles, with 'D' denoting the crystal size. The average crystal size was determined to be 28.9 nanometers, as calculated through the application of the Scherrer equation (16}, which utilizes the equation D=0.9$\lambda/\beta cos\theta$ to ascertain the crystal size.

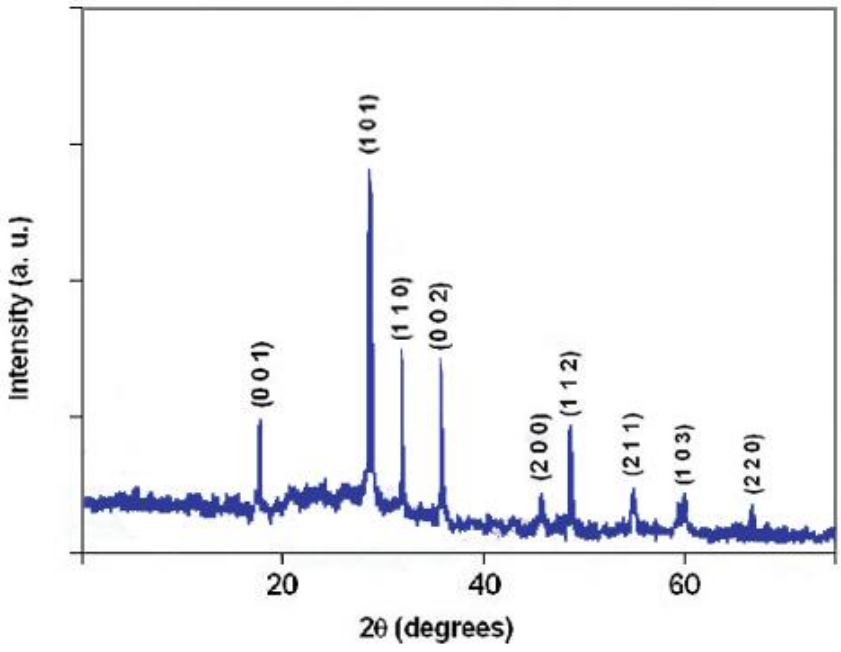

Figure 5: RXD spectrum of Pb

3.2.3 SEM of Pb-NPs

Figure 6 depicts the SEM image of Pb, captured using the SEM instrument. The illustration vividly displays the nanoparticles in a spherical configuration. Furthermore, these individual particles underwent clustering as part of the preparation procedure. The SEM image distinctly highlights the particles, revealing a well-defined, cohesive solid structure.

Several important factors, including the flow rate, reaction coil length, injection volume, and carrier stream pH, have an impact on the ISEs response when using the flow injection method. To confirm the accuracy of the findings, the impact of these criteria has thus been researched.

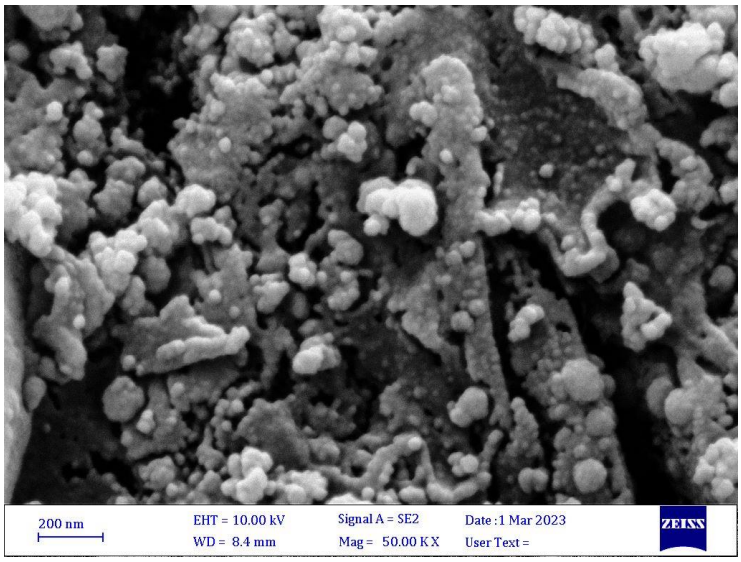

Figure 6: SEM image of Pb-NPs

3.3. Carrier current.

The FIA technique essentially needs a continuous carrier current solution. Therefore, a group of solutions with a concentration of 0.1 M (Perchlorate sodium, ammonium acetate, and potassium nitrate) by injecting a fixed volume of 150 µL of the sample at different concentrations and a constant flow speed, the obtained results showed that Perchlorate sodium 0.1 M gave the maximum peak and was chosen as the best carrier stream working with the Pb-NPs nanoelectrode. In contrast, alternative solutions resulted in a reduction in peak intensity and an upsurge in the consumption of chemicals. see Figure 7.

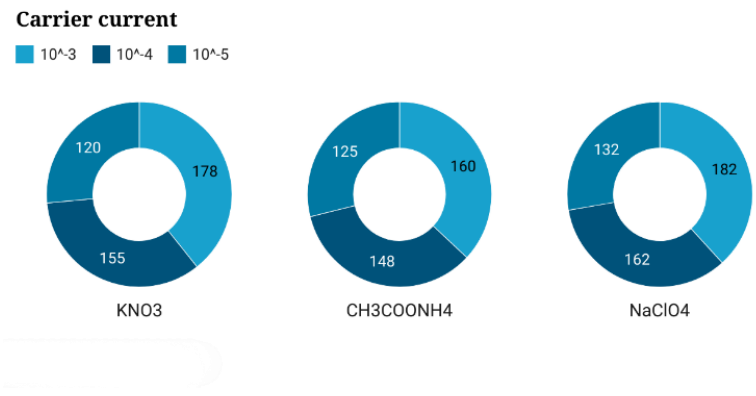

Figure 7: Carrier current solution.

3.4. *Flow rate influence.*

A wide range of flow rates, including 0.5, 0.8, 1, 1.6, 1.8, 2, and 2.5 mL/min, have been used to investigate the impact of flow rate on peak height. Figure 8 displays the findings of this experiment. This figure demonstrates that the Pb Nano electrode produced its maximum peak at a flow rate of 1.6 mL/min.

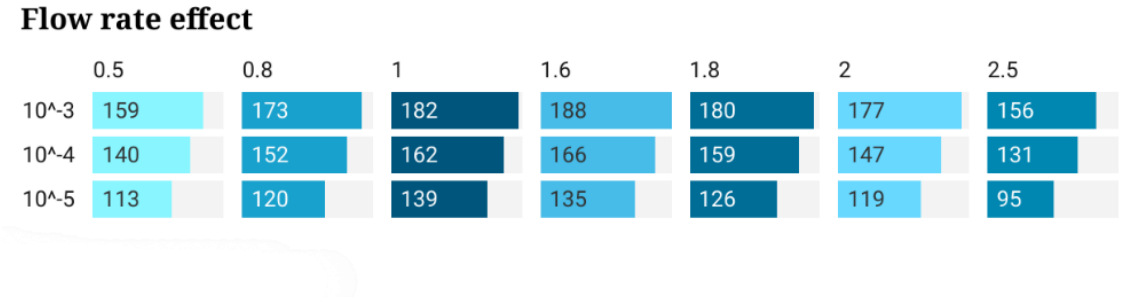

Figure 8: The influence of flow rate.

3.5. *Sample volume*

Different sample volumes (60, 90, 120, 150, 180 µL) were used to investigate the effect of injection volume, each containing a specific amount of ionic lead (1.00×10^{-3}, 1.00×10^{-4}, and 1.00×10^{-5} M). In the FIA system. The results presented in Figure 9 showed that the optimum volume for effective detection of ionic Lead was found to be 150 µL.

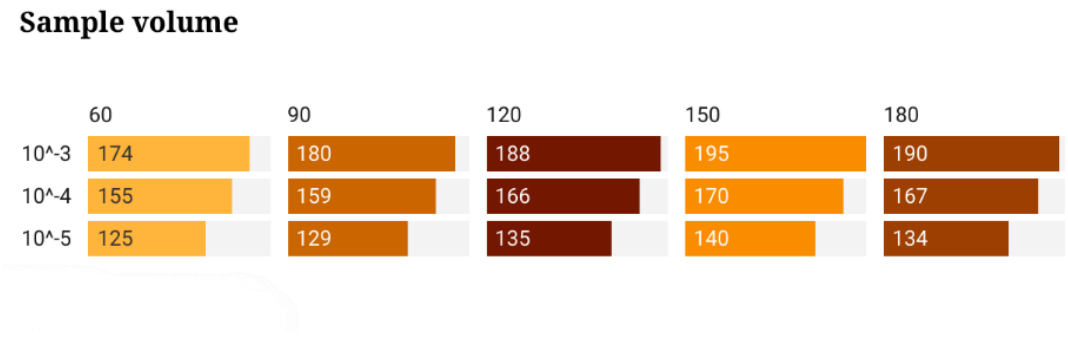

Figure 9: The injection volume, samples.

Table 1: Chemical and physical characteristics of the initial FIA experiment.

Parameters	Valve
Carrier stream	Perchlorate sodium0.1M
pH	5.1
Flow rate	1.6 mL/min
Inject sample value	150 µL
Reaction coil length	20 cm

3.7. *Calibration curve*

After testing the manufactured Nano electrode, a series of different concentrations of the lead ion solution was prepared, and measurements were taken under the selected optimal conditions. Each concentration was injected into the system three consecutive times. Then, the calibration curve was studied, representing the relationship between the change in voltage (expressed as peak height in millimeters) and the change in concentrations (expressed as -

log [ion]) as quantified in the Figure 10 and table 2. Through statistical data processing and using the necessary equations, linear regression (r^2), correlation coefficient, linear range (M), Lower detection (M), and Speed sample (hour).

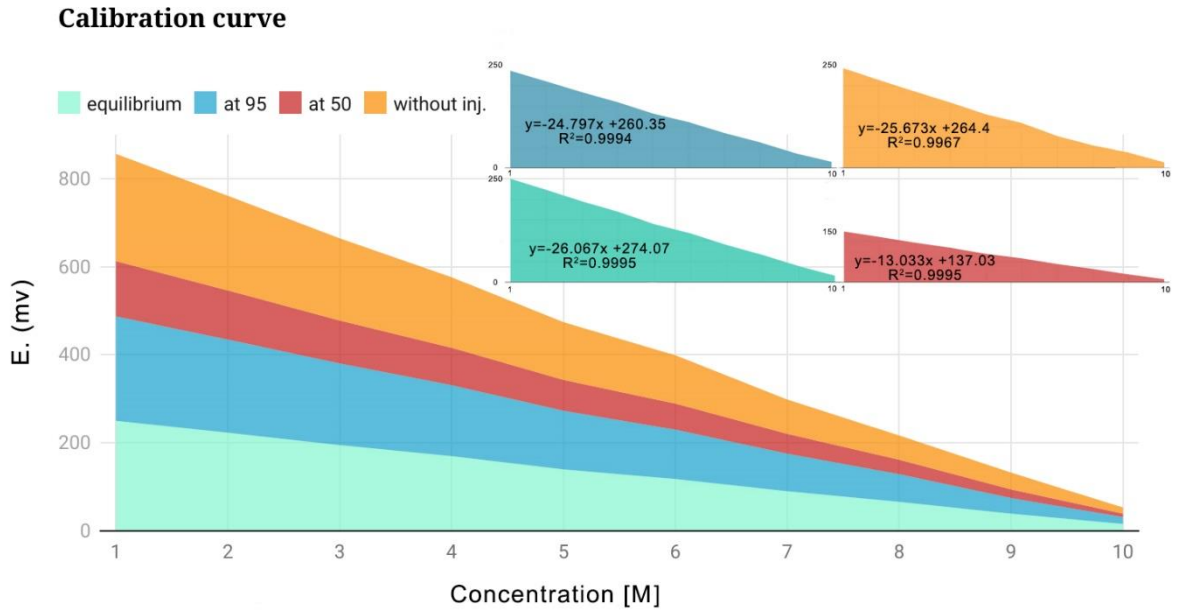

Figure 10: The nearest slope for the electrode, at equilibrium, 50, 95, and without injection.

Table 2. The properties of the electrode

Parameter	Pb-NPs Electrode
Regression equation	y = -26.067+ 274.06
Slope (mV. decade^{-1})	-26
Intercept	247.06
Linear range (M) .	1.00×10^{-1} - 1.00×10^{-10}
Relative coefficient	0.9980
Nernst response (M).	1.00×10^{-1}
Lower detection (M).	1.00×10^{-11}
Speed sample(hour)	120
Time	6 sec

3.8. Accuracy and precision.

After constructing the calibration curve for the manufactured Nano electrode, precision and accuracy were studied by injecting different concentrations of the ion to be measured into the carrier stream within the linear range of the calibration curve. These injections were performed consecutively under the selected optimal conditions. Table 3 shows that the percentage of recovery for the prepared electrode does not exceed 100.388%, and the highest value for the percentage of relative standard deviation for the electrode under study is 0.7863%. These results indicate that when using the electrode, high precision and accuracy are achieved. This study was carried out using Flow Injection Analysis (FIA) with translation technology.

Table 3: Accuracy and Precision

Electrode	Concentration (M)	Found	Theoretical	%RSD	%Rec	Mean
Pb-NPs	1.00×10^{-4}	170	169.8	0.3331	100.117	100.388
	1.00×10^{-6}	118	117.66	0.3461	100.286	
	1.00×10^{-8}	66	65.50	0.7863	100.763	

RSD: Relative Standard Deviation, Rec: Recovery.

3.9. Nearest slope electrode.

Table 4 and Figure 11 present a comparison between the theoretical Nernst slope and the measured slope (with and without injection) for the pb^{+2} electrode. This graph shows that the R2 value is consistently higher than 0.99. This value is admirable and shows that the theoretical and experimental slopes correspond quite well. (17-25).

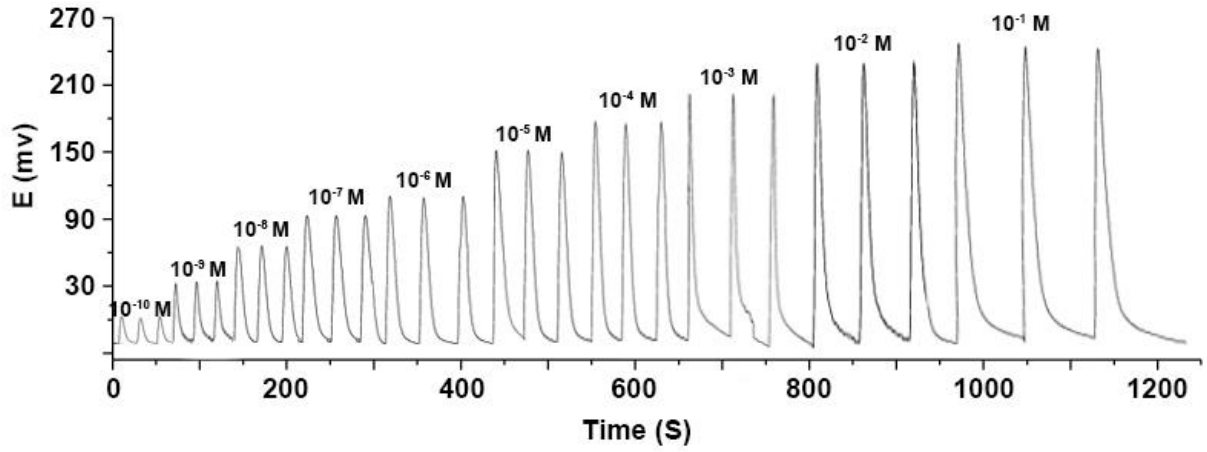

Figure 11: Recorder FIA response for Pb-NPs calibration at various concentrations and corresponding calibration graph.

Table 4: Nearest slope for the electrode.

Electrode	Speed	Concentration (M)	Without injection at t_{eq}	With injection at teq	Nernst theoretical slope
Pb-NPs	1.6ml/min	1.00×10^{-10}-1.00×10^{-1}	25	26	29

3.10. Determining the level of dispersion.

The highest initial response (H^o) was recorded after a concentration sample was passed without an injection, and the degree of dispersion was estimated using the equation below (26).

$$Log\ D = H^o - Hmax / S$$
$$S = 0.0951 / n$$

According to the findings, the electrode has a degree of dispersion of 2.37625, This is compatible with a dispersion coefficient (D) range of 1-3 and the use of polar ion sensitive detecting technologies. The type of dispersion is restricted (25). The outcomes are displayed in Table 5.

Table 5: The Nearest slope for the electrode.

Ele.	Con.(M)	H^o	H_{max}	Degree of dispersion	Mean
Pb-NPs	1.00×10^{-1}	250	261	2.5715	2.37625
	1.00×10^{-2}	223	240	2.7627	
	1.00×10^{-3}	195	205	2.53017	

	1.00×10^{-4}	170	182	2.60930	
	1.00×10^{-5}	140	155	2.71369	
	1.00×10^{-6}	118	131	2.65140	
	1.00×10^{-7}	90	101	2.57156	
	1.00×10^{-8}	66	78	2.60930	
	1.00×10^{-9}	39	53	2.67630	
	1.00×10^{-10}	16	25	2.59930	

Con.: Concentration, H^{o}: Initial concentration, $H_{max:}$ maximum height

3.11. Selective electrodes

Despite the sensitivity demonstrated by the lead Nano electrode, it is still susceptible to ion interferences. Therefore, the influence of the presence of certain positive ions and anions on its response was studied under the selected optimal conditions. The interference ratio was calculated using the equation (27), and the results are recorded in Tables 6. The results showed that some ions do not cause any interference.

Table 6: Potentiometric selectivity coefficients of several foreign ions on an electrode.

Ion of Pbs 0.01 (M)	Values $K_{i,j}^{pot}$	
	Ion Con. 0.1 (M)	Ion Con. 0.01 (M)
Br^{-1}	0.0015	0.0001
Cl^{-1}	0.0013	0.0009
K^{+1}	0.021	0.011
Cu^{+2}	0.0134	0.0021
Ca^{+2}	0.0243	0.0163
Fe^{+3}	0.114	0.165

3.12. Applications.

In this study, solid nano-electrodes were employed as detectors in the FIA to accurately determine lead concentrations in cosmetic products. First, 3 grams of each eye shadow sample (labeled as A) were precisely weighed using a balance and placed in individual clean, dry porcelain crucibles. To each sample, 3 ml of nitric acid was added. The crucibles were then heated on an electric heater until the samples were dry and subsequently allowed to cool. This process was repeated twice. After cooling, the crucibles were placed in an incineration furnace at a temperature of 522 °C for approximately two and a half hours, followed by a cooling period. Next, 3 ml of nitric acid was added to each sample, and the drying process was repeated twice using the electric heater, as described earlier. The samples were then filtered using glass cones and filter papers with a calibration of 0.05 ml. The experiment results are presented in Table 7 showing that lead ions from cosmetic products were collected in amounts ranging from 97.0% to 104.0%. (28).

Table 7: Application of the suggested method for measuring Pb-NPs in cosmetics (eye shadow).

Electrode	Color of an unknown sample	Unknown sample No.	Con. of the unknown sample(M)	original Con. Found (M)	%Rec
Pb-NPs	Brown	1	1.01×10^{-6}	1.00×10^{-6}	101.00
		2	9.82×10^{-5}	1.00×10^{-4}	98.20
		3	9.93×10^{-5}	1.00×10^{-4}	99.30

	Black	1	9.84×10^{-7}	1.00×10^{-6}	98.40
		2	9.78×10^{-6}	1.00×10^{-5}	97.80
		3	1.02×10^{-5}	1.00×10^{-5}	102.0
	Blue	1	1.03×10^{-3}	1.00×10^{-3}	103.0
		2	1.04×10^{-3}	1.00×10^{-3}	104.0
		3	9.92×10^{-5}	1.00×10^{-4}	99.20

Con.: Concentration, Rec: Recovery.

4. Conclusions

A straightforward and environmentally friendly method was developed using a green tea extract to manufacture a solid-state nano-electrode as a detector, utilizing the flow injection technique. Experimental work demonstrated that these electrodes are sensitive, stable, and selective. The nano-electrode exhibited excellent flow rates even with low injection volumes. The proposed methods are known for their simplicity, sensitivity, high specificity, and rapid measurement of lead ions in cosmetic preparations. Statistical analysis of the results confirmed the method's accuracy. Recommendations include exploring broader applications, optimizing manufacturing, collaborating with industries, and ensuring regulatory compliance.

References

1. Raju, C. Venkateswara, Rani, G. M., Haribabu, J., & Kumar, S. S. 2022. Flow Injection Analysis-Based Electrochemiluminescence: An Overview of Experimental Design and Its Biosensing Applications. *ECS Sensors Plus, 1*(3), 031604. https://doi.org/10.1149/2754-2726/ac8d70
2. Curulli, A., Lu, L., Fan, X., & Fan, Y. 2020. Nanomaterials in the Electrochemical Sensing Area: Applications and Challenges in Food Analysis. *Molecules*, *25*(23), 5759. https://doi.org/10.3390/molecules25235759
3. Gong, Z., Chan, H.T., Chen, Q., & Chen, H. 2021. Application of Nanotechnology in the Analysis and Removal of Heavy Metals in Food and Water Resources. *Nanomaterials (Basel), 11*(7), 1792. https://doi.org/10.3390/nano11071792
4. Sahragard, A., Varanusupakul, P., & Miró, M. 2023. Nanomaterial Decorated Electrodes in Flow-Through Electrochemical Sensing of Environmental Pollutants: A Critical Review. *Trends in Environmental Analytical Chemistry*, *39*, e00208. https://doi.org/10.1016/j.teac.2023.e00208
5. Hui, Y., Huang, Z., Alahi, M.E.E., Nag, A., Feng, S., & Mukhopadhyay, S.C. 2022. Recent Advancements in Electrochemical Biosensors for Monitoring Water Quality. *Biosensors (Basel)*, *12*(7), 551. https://doi.org/10.3390/bios12070551
6. Thomas, A. A., Varghese, R. M., & Rajeshkumar, S. 2022. Antimicrobial Effects of Copper Nanoparticles with Green Tea and Neem Formulation. *Bioinformation*, *18*(3), 284-288. https://doi.org/10.6026/97320630018284
7. Aswathi, V.P., Meera, S., Maria, C.G.A., et al. 2023. Green Synthesis of Nanoparticles from Biodegradable Waste Extracts and Their Applications: A Critical Review. *Nanotechnol. Environ. Eng*., *8*, 377-397. https://doi.org/10.1007/s41204-022-00276-8
8. Crisan, M.C., Teodora, M., & Lucian, M. 2022. Copper Nanoparticles: Synthesis and Characterization, Physiology, Toxicity, and Antimicrobial Applications. *Applied Sciences*, *12*, 141. https://doi.org/10.3390/app12010141
9. Keabadile, O.P., Aremu, A.O., Elugoke, S.E., & Fayemi, O.E. 2020. Green and Traditional Synthesis of Copper Oxide Nanoparticles - Comparative Study. *Nanomaterials (Basel)*, *10*(12), 2502. https://doi.org/10.3390/nano10122502
10. Ostad-Ali-Askari, K. 2022. Management of Risky Substances and Sustainable Development. *Applied Water Science*, *12*, 65. https://doi.org/10.1007/s13201-021-01562-7
11. Dhony, H., Nurul, I., Irmawanti, I., Ilfa, F., Diska, N., Khairi, Z. U., Handa, M., & Rahadi, W. 2023. Electrochemically Synthesized Biogenic Silver Nanoparticles Using Green Tea Extract as a Promising Antioxidant. *Karbala International Journal of Modern Science*, *9*(1), Article 8, 80-88. https://doi.org/10.33640/2405-609X.3276

12. Azizian-Kalandaragh, Y. 2018. Preparation of Lead Oxide Nanostructures in the Presence of Polyvinyl Alcohol (PVA) as a Capping Agent and Investigation of Their Structural and Optical Properties. *Journal of Semiconductor Technology and Science*, *18*(1), 91-99. https://doi.org/10.5573/jsts.2018.18.1.091
13. Trotte, N. S. F., Aben-Athar, M. T. G., & Carvalho, N. M. F. 2016. Yerba Mate Tea Extract: a Green Approach for the Synthesis of Silica Supported Iron Nanoparticles for Dye Degradation. *Journal of the Brazilian Chemical Society*, *27*(11), 2093-2104. https://doi.org/10.5935/0103-5053.20160100
14. Arulmozhi, K. T., & Mythili, N. 2013.Studies on the Chemical Synthesis and Characterization of Lead Oxide Nanoparticles with Different Organic Capping Agents. *AIP Advances*, *3*, 122122-1-9. https://doi.org/10.1063/1.4858419
15. Jayaramudu, T., Varaprasad, K., Kim, H. C., Kafy, A., Kim, J. W., & Kim, J. 2017. Calcinated tea and cellulose composite films and its dielectric and lead adsorption properties. *Carbohydrate Polymers*, *17*, 183-193. https://doi.org/10.1016/j.carbpol.2017.04.077
16. Guilbault, G., Durst, R., Frant, M., & Thomas, J. 1976. IUPAC Technical Reports and Recommendations. *Pure and Applied Chemistry*, *48*, 127. http://dx.doi.org/10.1351/pac197648010127
17. Mardle, P., Cerri, I., Suzuki, T., & El-kharouf, A. 2021. An Examination of the Catalyst Layer Contribution to the Disparity between the Nernst Potential and Open Circuit Potential in Proton Exchange Membrane Fuel Cells. *Catalysts*, *11*, 965. https://doi.org/10.3390/catal11080965
18. Pallant, J. SPSS Survival Manual (2nd ed.). Australia: Allen & Unwin. 2005. Page 318.
19. Abdulredha, M., Al Khaddar, R., Jordan, D., Kot, P., Abdulridha, A., & Hashim, K. 2018. Estimating solid waste generation by the hospitality industry during major festivals: A quantification model based on multiple regression. *Waste Management*, *77*, 388-400. https://doi.org/10.1016/j.wasman.2018.04.025
20. Abdulredha, M., Rafid, A., Jordan, D., & Hashim, K. 2017. The development of a waste management system in Kerbala during major pilgrimage events: determination of solid waste composition. *Procedia Engineering*, *196*, 779-784. https://doi.org/10.1016/j.proeng.2017.08.007
21. Alattabi, A. W., Harris, C., Alkhaddar, R., Alzeyadi, A., & Hashim, K. s' Wastewater using Environmentally Friendly Technology. *Procedia Engineering*, 2017. Treatment of Residential Complexe *196*, 792-799. https://doi.org/10.1016/j.proeng.2017.08.009
22. Alattabi, A. W., Harris, C. B., Alkhaddar, R. M., Hashim, K. S., Ortoneda-Pedrola, M., & Phipps, D. 2017. Improving sludge settleability by introducing an innovative, two-stage settling sequencing batch reactor. *Journal of Water Process Engineering*,. *20*, 207-216. https://doi.org/10.1016/j.jwpe.2017.11.004
23. Shubbar, A. A., Jafer, H., Dulaimi, A., Hashim, K., Atherton, W., & Sadique, M. 2018. The development of a low carbon binder produced from the ternary blending of cement, ground granulated blast furnace slag, and high calcium fly ash: An experimental and statistical approach. *Construction and Building Materials*, *187*, 1051-1060. https://doi.org/10.1016/j.conbuildmat.2018.08.021
24. Hashim, K.S., Al-Saati, N.H., Hussein, A.H., & Al-Saati, Z.N. 2018. An Investigation into the Level of Heavy Metals Leaching from Canal-Dredged Sediment: A Case Study on Metals Leaching from Dredged Sediment. IOP Conference Series: *Materials Science and Engineering*, *454*, Article ID: 012022. doi: 10.1088/1757-899X/454/1/012022.
25. Ružička, J., & Hansen, E. 1975. Flow injection analyses: Part I. A new concept of fast continuous flow analysis. *Analytica Chimica Acta*, *78*(1), 145-157.
26. Al Samarrai, S. Y., Abdoon, F. M., & Hashim, K. K. 2019. A simple method to determine tramadol using a coated-wire electrode as a detector in the flow injection analysis. *Microchemical Journal*, *146*, 588-591. https://doi.org/10.1016/j.microc.2019.01.041
27. Guilbault, G., Durst, R., Frant, M., & Thomas, J. 1976. IUPAC Technical Reports and Recommendations. *Pure and Applied Chemistry*, *48*, 127.

28. Maharaj, D., Mohammed, T., Mohammed, A., & Addison, L. *2021*. Enhanced digestion of complex cosmetic matrices for analysis of As, Hg, Cd, Cr, Ni, and Pb using Triton X-100. *MethodsX*, *8*, 101241. https://doi.org/10.1016/j.mex.2021.101241.